Age-Dependent Changes in Regulation of Water Inflow Into the Vitreous Body

Satoshi Ueki,[1,2] Yuji Suzuki,[1] Yukimi Nakamura,[1] and Hironaka Igarashi[1]

[1]Center for Integrated Human Brain Science, Brain Research Institute, Niigata University, Niigata, Japan
[2]Division of Ophthalmology and Visual Science, Graduate School of Medical and Dental Sciences, Niigata University, Niigata, Japan

Correspondence: Yuji Suzuki, Center for Integrated Human Brain Science, Brain Research Institute, Niigata University, Asahimachi-dori 1-757, Chuo-ku, Niigata 951-8585, Japan; yuji-s@bri.niigata-u.ac.jp.

Received: April 12, 2023
Accepted: August 22, 2023
Published: September 12, 2023

Citation: Ueki S, Suzuki Y, Nakamura Y, Igarashi H. Age-dependent changes in regulation of water inflow into the vitreous body. *Invest Ophthalmol Vis Sci.* 2023;64(12):22. https://doi.org/10.1167/iovs.64.12.22

Purpose. Water inflow into the vitreous body regulated by retinal aquaporin-4 distributed within Müller cells has been observed in mice; however, the changes in this phenomenon with age remain unknown. This study aimed to evaluate whether intravenously injected H_2O also flows into the vitreous body of human subjects and to investigate whether water dynamics in the human posterior eye change with age using [^{15}O]H_2O positron emission tomography (PET).

Methods. Forty-six normal adult volunteers underwent [^{15}O]H_2O PET, and the standard uptake value (SUV) in the center of the vitreous body after 1000-MBq [^{15}O]H_2O administration was assessed. The SUV was fitted to an exponential curve, and y_0, the steady state of the SUV, and b, the speed of increase in the SUV, were calculated. The results for patients ranging from in age from 20 to 39, 40 to 59, and 60 to 79 years were compared using analyses of variance followed by Games to Howell tests.

Results. For the parameter y_0, statistical analysis revealed no statistically significant differences among the three groups. For parameter b, statistical analysis revealed statistically significant differences between the 20 to 39 and 60 to 79 age groups ($P = 0.000$), the 40 to 59 and 60 to 79 age groups ($P = 0.025$), and the 20 to 39 and 40 to 59 age groups ($P = 0.037$).

Conclusions. The present study revealed that H_2O injected into the vein flows into the human vitreous body and that the speed of increase in water flow into the vitreous body decreases with aging. This study suggests that water dynamics in the posterior eye, or the retinal glymphatic pathway, change significantly with aging.

Keywords: aging, positron emission tomography, post-iridial flow, retinal glymphatic pathway, aquaporin-4

Aquaporin-4 (AQP4) is abundantly distributed in the ocular tissue,[1] and, specifically within the retina, it has the potential to regulate water dynamics in the posterior eye. The regulation of water inflow into the vitreous body in mice was evaluated using JJ vicinal coupling proton exchange magnetic resonance imaging (JJVCPE MRI) with $H_2{}^{17}O$, a non-radioactive isotope.[2] The study showed that $H_2{}^{17}O$ injected into the femoral vein of mice flowed into the vitreous body as a part of the aqueous humor (i.e., post-iridial flow),[3–5] and the absorption of water into the retina was impaired in AQP4 knockout mice. It can be assumed that this phenomenon, which involves water dynamics in the posterior eye regulated by retinal AQP4 distributed within the Müller cells, could occur in humans, as well. We have referred to the water dynamics in the posterior eye as the retinal glymphatic pathway, drawing an analogy with the glymphatic pathway in the cerebrum, which is responsible for the removal of waste substances such as β-amyloid.[6,7]

For regulation of the cerebral glymphatic pathway, AQP4 present at the endfeet of astrocytes plays a major role.[8] Although there are significant findings regarding the cerebral glymphatic pathway, little is known about its role in the retinal glymphatic pathway. However, it has been reported that the efficiency of cerebral glymphatic pathway decreases with age and is also impaired in patients with Alzheimer's disease, which is more prevalent in the elderly, using positron emission tomography (PET) with [^{15}O]H_2O, a radioactive isotope, to demonstrate the reduced water inflow into the cerebrospinal fluid space.[9] Considering the fact that the prevalence of certain ocular diseases increases in the elderly, similar changes may occur in these diseases, such as in Alzheimer's disease.

Regarding the aforementioned analogy between the glymphatic pathways of the retina and the cerebrum, the lack of findings regarding age-related changes in the retinal glymphatic pathway is a significant gap. In particular, the accumulation of β-amyloid might be associated with the pathogenesis of glaucoma and age-related macular degeneration,[10–12] which are among the most prevalent ocular diseases in the elderly. Animal studies have shown that intraocular pressure elevation can lead to the accumulation of β-amyloid in the retina, optic nerve, and lateral geniculate body.[10,11] Dentchev et al.[12] reported the presence of β-amyloid in drusen among four out of nine eyes affected

by age-related macular degeneration. In Alzheimer's disease, impairment of the cerebral glymphatic pathway may facilitate β-amyloid accumulation. This suggests that, similar to the cerebrum, the retinal glymphatic pathway becomes progressively impaired with aging, and the efficiency of waste product clearance is greatly reduced. An in-depth study of these age-related changes will provide an opportunity to clarify the relationship between the retinal glymphatic pathway and ocular diseases, the incidence of which increases with age, and thereby elucidate the pathogenic mechanism.

Although there is no established method to measure water dynamics in the human posterior eye, $[^{15}O]H_2O$ PET may help assess the same in the human posterior eye to a great extent. This technique has been clinically used in humans. In the present study, we evaluated whether intravenously injected H_2O also flows into the vitreous body in human subjects using $[^{15}O]H_2O$ PET and investigated whether water dynamics in the human posterior eye change with aging.

Methods

Forty-six healthy adult volunteers (32 males and 14 females) participated in this study. The volunteers were 20 to 79 years old (16 volunteers, 20–39 years; 10 volunteers, 40–59 years; and 20 volunteers, 60–79 years). All participants were asked if they had any significant medical conditions, such as chronic heart, kidney, pulmonary, and ophthalmologic diseases, and if they were free of these conditions. The study protocol was explained in detail to all participants, and written informed consent was obtained. All participants were provided with contact names and telephone numbers in the event of any adverse event related to the study. Within 1 month of each PET image, we confirmed the absence or occurrence of study-related adverse events in all participants. This study was approved by the Institutional Review Board/Ethics Committee of Niigata University and followed the tenets of the Declaration of Helsinki. This $[^{15}O]H_2O$ PET study was registered in the UMIN Clinical Trials Registry (UMIN000011939).

A combined PET/computed tomography (CT) scanner (Discovery ST Elite; GE Healthcare, Schenectady, NY, USA) was used for all of the $[^{15}O]H_2O$ PET scans. The scanner had an axial field of view (FOV) of 15 cm in the head region, including both eyes. To correct photon attenuation, a low-dose CT scan was acquired in helical mode with the following parameters: 120 kV, 50 mA, 0.8 seconds per tube rotation, slice thickness of 3.75 mm with intervals of 3.27 mm, pitch of 0.875, and a table speed of 17.5 mm/rotation. During the

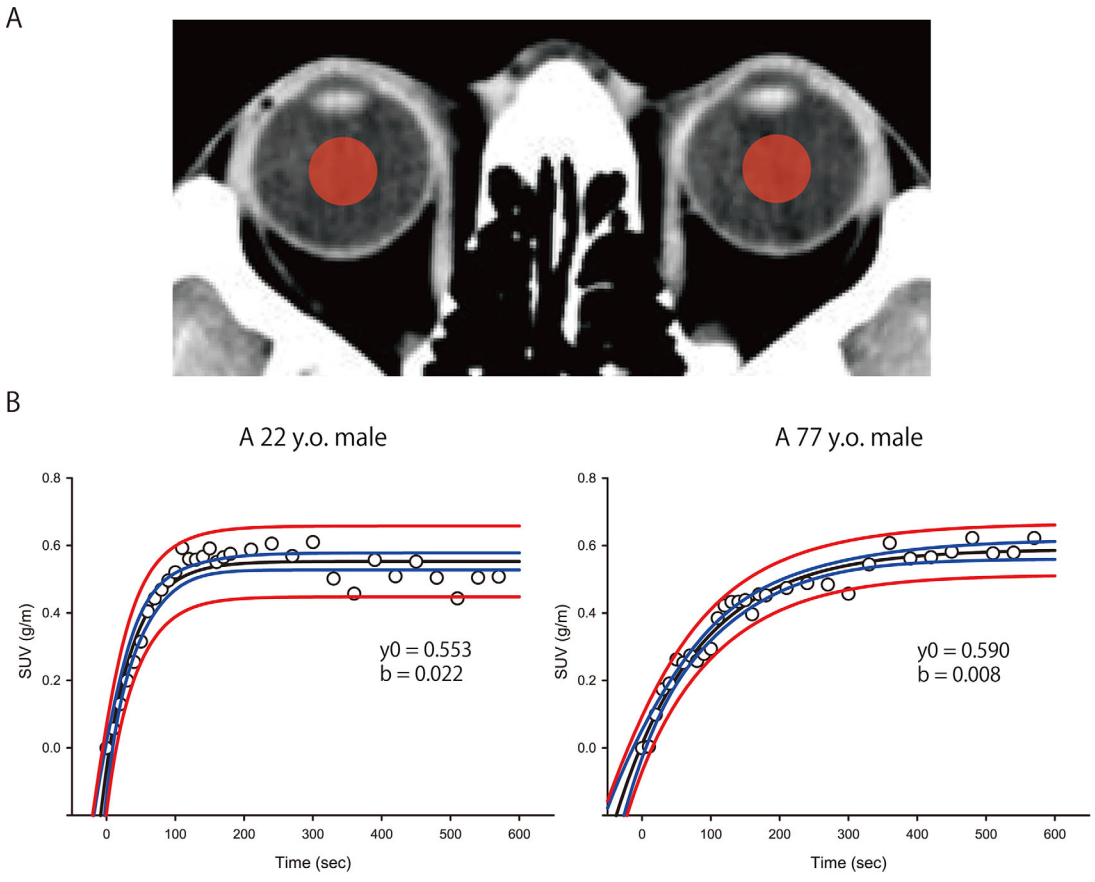

Figure 1. Results of $[^{15}O]H_2O$ positron emission tomography (PET) of the eyes in normal adult volunteers. (**A**) The circular region of interest was set to include the center of the eye containing the vitreous body (*red-filled circles*). (**B**) Increases in the SUV after administration of 1000-MBq $[^{15}O]H_2O$ as observed in a 22-year-old male and a 77-year-old male. The time course of the SUV in the center of the vitreous body was fitted from the start point to the following exponential curve: $y(t) = y_0 + ae^{-bt}$ The results of the fitting, obtained using SigmaPlot 14.5, are presented as follows: calculated y_0, calculated b, fitted curve (*black line*), 95% confidence band (shown between *blue lines*), and 95% prediction band (shown between *red lines*). SUV, standard uptake value.

Investigative Ophthalmology & Visual Science

scanning procedure, the participant's head was rested on a foam-cushioned headrest, and a head strap was used to minimize unwanted movement. Participants were instructed to close their eyes and minimize eye movement during the scanning procedure. For each PET scan, 1000 MBq of $[^{15}O]H_2O$ was produced online and injected intravenously (AM WR01; JFE Technos, Yokohama, Japan). The AM WR01 delivered a 10-mL bolus at a speed of 1 mL/s with pre- and post-flushing of an inert saline solution. All PET emission scans were normalized to the detector inhomogeneity and corrected for random coincidence, dead time, scattered radiation, and photon attenuation. Dynamic images were reconstructed using a three-dimensional (3D) ordered-subset expectation maximization with two iterations and 28 subsets to obtain superior visual quality images. After initiating the injection, PET emission data were promptly acquired over 10 minutes in 3D list mode with a 25.6-cm axial FOV and were collected in a 128 × 128 × 47 matrix with a voxel size of 2.0 × 2.0 × 3.75 mm.

Both CT and PET image data were transferred to a Xeleris 3.1 workstation (GE Healthcare) and regions of interest (ROIs; center of the vitreous body in both eyes) were manually defined using Volumetrix MI (GE Healthcare) on the workstation (Fig. 1A). The ROI size was 20 voxels in one eye (the volume was 300.0 mm^3). The tissue activity concentration in each ROI was expressed as a standardized uptake value (SUV; g/mL), which was corrected for each participant's body weight and administered dose of radioactivity. Data were obtained every 10 seconds from the start point to 180 seconds and then every 30 seconds from 210 to 600 seconds. Each time course of tissue activity concentration was fitted from the starting point in the ROI to the following exponential curve using SigmaPlot 14.5 (Systat Software, Chicago, IL, USA) (Fig. 1B):

$$y(t) = y_0 + ae^{-bt}$$

Here, y_0 and b in each tissue implied steady state of the SUV and the speed of increase of the SUV reflecting the in/out flow pace, respectively.[13]

Statistical analyses, including analysis of variance (ANOVA) followed by Games–Howell to compare numerical data, y_0 and b, among the three groups (20–39, 40–59, and 60–79 years), were performed using SPSS Statistics 19.0 (IBM, Chicago, IL, USA), and P values less than 0.05 were regarded as statistically significant. The mean values for both eyes were used.

Results

All 46 healthy volunteers undergoing $[^{15}O]H_2O$ PET showed an increase in the SUV after 1000-MBq $[^{15}O]H_2O$ administration. Time courses of the SUVs for all participants and those of the mean SUVs of the 20 to 39, 40 to 59, and 60 to 79 years age groups are shown in Figure 2. For parameter y_0, mean values with standard deviations (SDs) were 0.456 ± 0.048 for 20 to 39 years, 0.432 ± 0.026 for 40 to 59 years, and 0.422 ± 0.062 for 60 to 79 years. Statistical analysis revealed no significant differences between the three groups (Fig. 3A). For parameter b, mean values with SDs were 0.017 ± 0.003 for 20 to 39 years, 0.014 ± 0.003 for 40 to 59 years, and 0.010 ± 0.004 for 60 to 79 years. Statistical analysis revealed significant differences between the 20 to 39 and 60 to 79 age groups (P = 0.000), the 40 to 59 and 60 to 79 age groups (P = 0.025), and the 20 to 39 and 40 to 59 age groups (P = 0.037) (Fig. 3B).

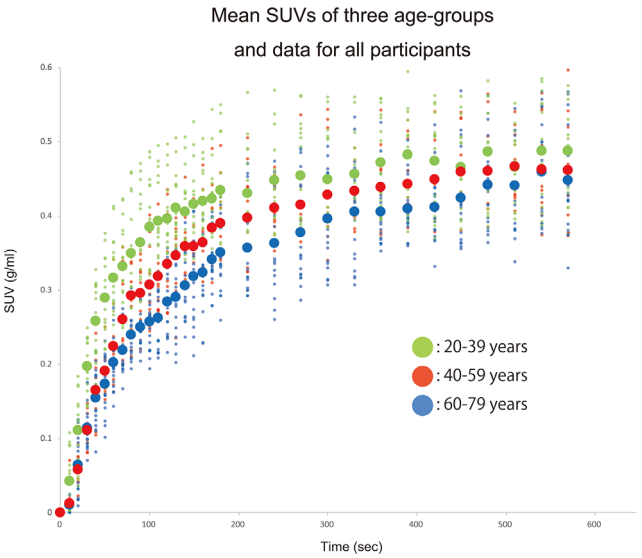

Figure 2. Increase in the SUVs after administration of 1000-MBq $[^{15}O]H_2O$ as observed in all participants. The SUVs of all participants are represented as *small filled circles*. Mean SUVs for the age groups of 20 to 39, 40 to 59, and 60 to 79 years are represented as *large filled circles*. *Green circles* represent the values of the 20 to 39 years age group, *red circles* represent those of the 40 to 59 years age group, and *blue circles* represent those of the 60 to 79 years age group.

Discussion

In this study, we showed that intravenously injected H_2O flows into the vitreous body in humans using $[^{15}O]H_2O$ PET. These findings suggest that the post-iridial flow observed in mice, wherein water administered through the femoral vein flows into the vitreous body, also occurs in humans. Moreover, if the human eye possessed mechanisms similar to those observed in mice, this post-iridial flow in humans would have been reabsorbed into the retina, just as seen in mice. JJVCPE MRI with $H_2{}^{17}O$ is an expensive technique because of the low relative isotopic abundance of ^{17}O; therefore, it has not yet been established as a feasible methodology for human evaluation. In contrast, the present study employed $[^{15}O]H_2O$ PET, a methodology that has been utilized for a considerable period in the assessment of cerebral blood flow.[14,15] Considering the fact that this method directly observes water, we believe that it can be applied to evaluate water dynamics in the posterior eye of humans.

We analyzed the time–activity concentration of the vitreous body by applying the equation described in the Methods section to the temporal changes in the SUV of $[^{15}O]H_2O$ in the vitreous body. For parameter b, which can be considered as the speed of increase in SUV, there were statistically significant reductions with aging between the age groups of 20 to 39 and 60 to 79 years, 40 to 59 and 60 to 79 years, and 20 to 39 and 40 to 59 years. However, for parameter y_0, which can be considered a steady state of the SUV, there were no statistically significant differences among the three groups. As discussed in the study on mice using JJVCPE MRI with $H_2{}^{17}O$, the influx of water into the vitreous body is mainly controlled by the

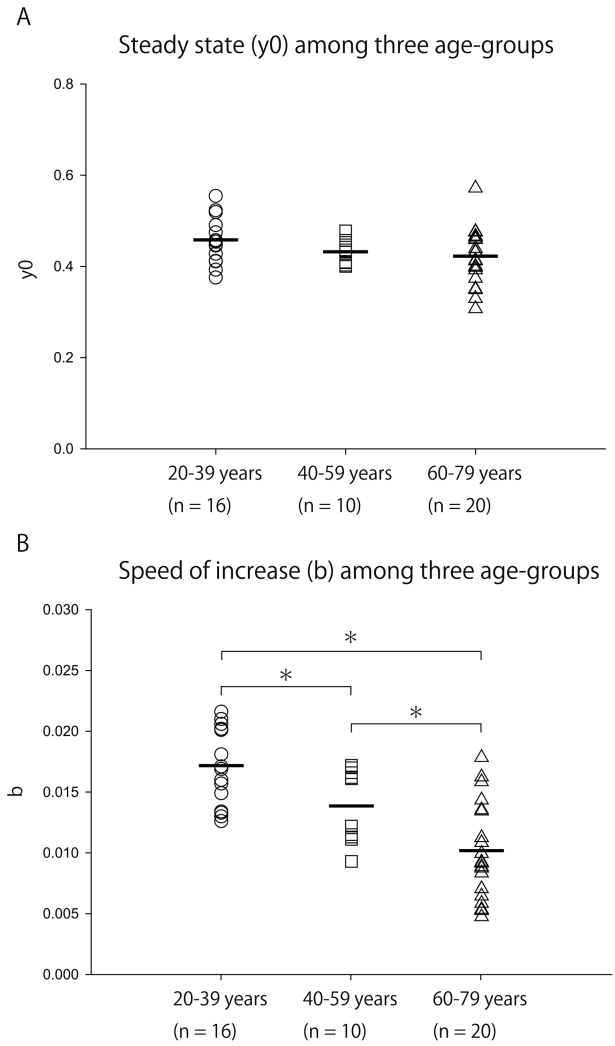

Figure 3. Parameters y_0 and b among the age groups of 20 to 39, 40 to 59, and 60 to 79 years. Parameters y_0 and b as calculated from below: time course of SUV in the center of the vitreous body was fitted from the start point to the following exponential curve: $y(t) = y_0 + ae^{-bt}$ (**A**) Parameter y_0 is the steady state of SUV among the three groups. There are no statistically significant differences among the groups. (**B**) Parameter b is the speed of increase in the SUV among the three groups. Statistically significant differences were observed between the 20 to 39 and 60 to 79 years age groups ($P = 0.000$), the 40 to 59 and 60 to 79 years age groups ($P = 0.025$), and the 20 to 39 and 40 to 59 years age groups ($P = 0.037$). The *bars* represent mean values. *$P < 0.05$, ANOVA followed by the Games–Howell test.

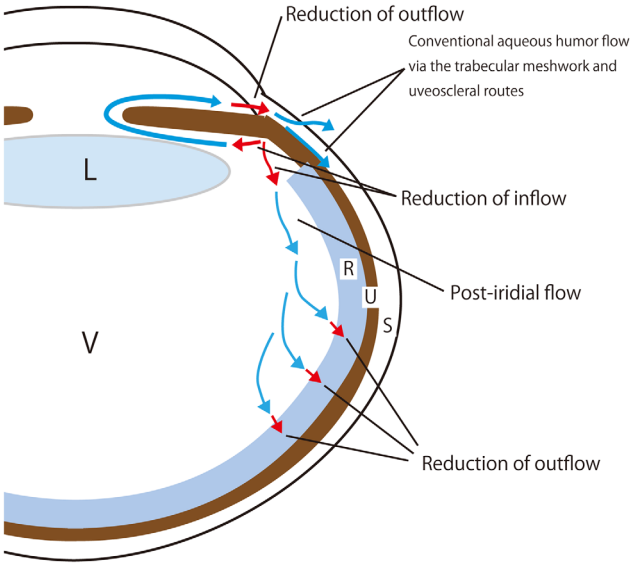

Figure 4. Presumed mechanisms explaining the results of the present study. Herein, the speed of increase in SUV changed with aging, whereas the steady state of the SUV remained unchanged. These results can be interpreted by a reduction of water inflow into the vitreous body due to the age-related decrease in aqueous humor production and reduction of water outflow from the vitreous body due to the age-related decrease in absorption into the retina (*red arrows*). Additionally, age-related decreases in conventional aqueous humor inflow and outflow via the trabecular meshwork and uveoscleral routes may influence these results (*red arrows*). L, lens; R, retina; S, sclera; U, uvea; V, vitreous body.

aqueous humor produced at the ciliary epithelium, and the outflow from the vitreous body is mainly controlled by its absorption into the retina.[2] The results of this study show that the speed of increase in SUV changes with aging, whereas the steady state of SUV remains unchanged, suggesting the possibility that water inflow into the vitreous body decreases due to the age-related reduction in the aqueous humor production, and that the water outflow from the vitreous body also decreases due to the age-related reduction in its absorption into the retina. These possibilities suggest that decreased water inflow into the vitreous body may mask age-related reductions in water absorption into the retina (Fig. 4). The former is supported by the finding that the production of aqueous humor decreases with age.[16,17] The latter is supported by the finding that water dynamics in the brain decrease with age.[9] Additionally, conventional aqueous humor outflow via the trabecular meshwork and uveoscleral routes decreases with aging.[16] Although in this study we examined inflow and outflow within the vitreous body in this study, it is important to note that the reduction of conventional outflow may influence the measurement results to some extent.

AQP4, which is abundantly distributed in ocular tissue, has a potential role in regulating water dynamics in the posterior eye. In fact, in AQP4 knockout mice, water influx into the retina is impaired.[2] Zeppenfeld et al.[18] reported that AQP4 expression in the human brain is altered in aging brains; the ratio of AQP4-M1 to AQP4-M23, as analyzed by western blotting, declined in the aged cortex. Similar changes are expected to occur in the posterior eye, suggesting that the function of AQP4 in retinal Müller cells declines with aging. Accordingly, the key to revealing these expected findings in detail is to analyze whether the expression of AQP4 within retinal Müller cells changes with age. Future research may lead to the discovery of new methods for the treatment and prevention of age-related ocular diseases.

In this study, to minimize the influence of eye movement, the subjects' heads were fixed, and they were instructed to close their eyes during the test. The ROI was set at the center of the vitreous body to ensure accurate data acquisition. Although further improvement is needed to obtain more accurate data, it is considered sufficient to observe water dynamics in the posterior eye.

The present study revealed that H_2O injected into the vein flows into the vitreous body in humans and that the speed of

Investigative Ophthalmology & Visual Science

increase in water flow into the vitreous body decreases with aging. These results suggest that the water dynamics in the posterior eye, also known as the retinal glymphatic pathway, change with aging, and future analysis of $[^{15}O]H_2O$ PET in patients with glaucoma, age-related macular degeneration, and other ocular diseases more prevalent in the elderly may clarify the relationship between these ocular diseases and the retinal glymphatic pathway.

Acknowledgments

A review published by Nakada et al.[7] has illuminated our path forward. Unfortunately, Professor Nakada passed away in July 2018.

Supported by grants from the Ministry of Education, Culture, Sports, Science and Technology (Japan) and Japan Society for the Promotion of Science (JSPS) KAKENHI (JP1122086 and JP1141675).

Disclosure: **S. Ueki**, None; **Y. Suzuki**, None; **Y. Nakamura**, None; **H. Igarashi**, None

References

1. Verkman AS, Ruiz-Ederra J, Levin MH. Functions of aquaporins in the eye. *Prog Retin Eye Res*. 2008;27(4):420–433.
2. Ueki S, Suzuki Y, Igarashi H. Retinal aquaporin-4 and regulation of water inflow into the vitreous body. *Invest Ophthalmol Vis Sci*. 2021;62(2):24.
3. Araie M, Maurice DM. The loss of fluorescein, fluorescein glucuronide and fluorescein isothiocyanate dextran from the vitreous by the anterior and retinal pathways. *Exp Eye Res*. 1991;52(1):27–39.
4. Araie M, Sugiura Y, Sakurai M, Oshika T. Effect of systemic acetazolamide on the fluid movement across the aqueous-vitreous interface. *Exp Eye Res*. 1991;53(3):285–293.
5. Tsuboi S. Measurement of the volume flow and hydraulic conductivity across the isolated dog retinal pigment epithelium. *Invest Ophthalmol Vis Sci*. 1987;28(11):1776–1782.
6. Nakada T, Kwee IL, Igarashi H, Suzuki Y. Aquaporin-4 functionality and Virchow-Robin space water dynamics: physiological model for neurovascular coupling and glymphatic flow. *Int J Mol Sci*. 2017;18(8):1798.
7. Nakada T, Kwee IL. Fluid dynamics inside the brain barrier: current concept of interstitial flow, glymphatic flow, and cerebrospinal fluid circulation in the brain. *Neuroscientist*. 2019;25(2):155–166.
8. Orešković D, Klarica M. The formation of cerebrospinal fluid: nearly a hundred years of interpretations and misinterpretations. *Brain Res Rev*. 2010;64(2):241–262.
9. Suzuki Y, Nakamura Y, Yamada K, et al. Reduced CSF water influx in Alzheimer's disease supporting the β-amyloid clearance hypothesis. *PLoS One*. 2015;10(5):e0123708.
10. Yan Z, Liao H, Chen H, et al. Elevated intraocular pressure induces amyloid-β deposition and tauopathy in the lateral geniculate nucleus in a monkey model of glaucoma. *Invest Ophthalmol Vis Sci*. 2017;58(12):5434–5443.
11. Ito Y, Shimazawa M, Tsuruma K, et al. Induction of amyloid-β(1-42) in the retina and optic nerve head of chronic ocular hypertensive monkeys. *Mol Vis*. 2012;18:2647–2657.
12. Dentchev T, Milam AH, Lee VMY, Trojanowski JQ, Dunaief JL. Amyloid-β is found in drusen from some age-related macular degeneration retinas, but not in drusen from normal retinas. *Mol Vis* 2003;9:184–190.
13. Suzuki Y, Nakamura Y, Igarashi H. Blood cerebrospinal fluid barrier function disturbance can be followed by amyloid-β accumulation. *J Clin Med*. 2022;11(20):6118.
14. Raichle ME, Martin WR, Herscovitch P, Mintun MA, Markham J. Brain blood flow measured with intravenous $H_2{}^{15}O$. II. Implementation and validation. *J Nucl Med*. 1983;24(9):790–798.
15. Lammertsma AA, Cunningham VJ, Deiber MP, et al. Combination of dynamic and integral methods for generating reproducible functional CBF images. *J Cereb Blood Flow Metab*. 1990;10(5):675–686.
16. Gabelt BT, Kaufman PL. Changes in aqueous humor dynamics with age and glaucoma. *Prog Retin Eye Res*. 2005;24(5):612–637.
17. Toris CB, Yablonski ME, Wang YL, Camras CB. Aqueous humor dynamics in the aging human eye. *Am J Ophthalmol*. 1999;127(4):407–412.
18. Zeppenfeld DM, Simon M, Haswell JD, et al. Association of perivascular localization of aquaporin-4 with cognition and Alzheimer disease in aging brains. *JAMA Neurol*. 2017;74(1):91–99.

Investigative Ophthalmology & Visual Science